Biol. Cybern. 91, 159–167 (2004)
DOI 10.1007/s00422-004-0495-1

Biological Cybernetics

Spike timing and synaptic plasticity in the premotor pathway of birdsong

Henry D. I. Abarbanel[1,2], **Leif Gibb**[3], **Gabriel B. Mindlin**[3,4], **M. I. Rabinovich**[2], **Sachin Talathi**[1,3]

[1] Department of Physics, and Marine Physical Laboratory (Scripps Institution of Oceanography), University of California, San Diego, 9500 Gilman Drive, La Jolla, CA 92093-0402, USA
[2] Center for Theoretical Biological Physics, University of California, San Diego, 9500 Gilman Drive, La Jolla, CA 92093-0402, USA
[3] Institute for Nonlinear Science, University of California, San Diego, 9500 Gilman Drive, La Jolla, CA 92093-0402, USA
[4] Departamento de Física, Facultad de Ciencias Exactas y Naturales, Universidad de Buenos Aires, Ciudad Universitaria, Pabellon I (1428), Buenos Aires, Argentina

Received: 25 September 2003 / Accepted: 27 May 2004 / Published online: 10 September 2004

Abstract. The neural circuits of birdsong appear to utilize specific time delays in their operation. In particular, the anterior forebrain pathway (AFP) is implicated in an approximately 40- to 50-ms time delay, ΔT, playing a role in the relative timing of premotor signals from the nucleus HVc to the nucleus robust nucleus of the archistratium (RA) and control/learning signals from the nucleus lateral magnocellular nucleus of the anterior neostratium (lMAN) to RA. Using a biophysical model of synaptic plasticity based on experiments on mammalian hippocampal and neocortical pyramidal neurons, we propose an understanding of this $\approx$ 40- to 50-ms delay. The biophysical model describes the influence of Ca^{2+} influx into the postsynaptic RA cells through NMDA and AMPA receptors and the induction of LTP and LTD through complex metabolic pathways. The delay, ΔT, between HVc $\rightarrow$ RA premotor signals and lMAN $\rightarrow$ RA control/learning signals plays an essential role in determining if synaptic plasticity is induced by signaling from each pathway into RA. If ΔT is substantially larger than 40 ms, no plasticity is induced. If ΔT is much less than 40 ms, only potentiation is expected. If $\Delta T \approx 40$ ms, the sign of synaptic plasticity is sensitive to ΔT. Our results suggest that changes in ΔT may influence learning and maintenance of birdsong. We investigate the robustness of this result to noise and to the removal of the Ca^{2+} contribution from lMAN $\rightarrow$ RA NMDA receptors.

1 Introduction

Birdsong is a rich test bed for the study of the learning of complex behavior. The genetic constraints on song are sufficiently loose in oscine songbirds, hummingbirds, and parrots that development of normal song requires a process of imitative learning (Nottebohm 2002). Songbirds pass through a sensory phase, in which young birds memorize a tutor song, and a sensorimotor phase, in which they gradually learn to match their own vocalizations to the memorized tutor song. At the end of the sensorimotor phase, the song undergoes crystallization and becomes stable (Brainard and Doupe 2002; Konishi 1965, 1985). The neural substrates for birdsong are usually described in terms of different pathways: well-differentiated sets of neurons, nuclei, which are interconnected in precise ways. In oscines, these nuclei have been thoroughly studied (Brenowitz et al. 1997).

The motor pathway generates and coordinates the patterned activity necessary for song production (Brainard and Doupe 2002). Its main nuclei are HVc and RA. HVc contains RA-projecting neurons firing sparse bursts of spikes (Hahnloser et al. 2002). In each motif of birdsong, lasting about 1 s, each RA-projecting HVc neuron fires one burst of 4.5 ± 2 spikes in a window of 6.1 ± 2 ms. A sequence of HVc neurons bursting in this sparse way excites a subpopulation of neurons in the RA nucleus, some of which project onto motor neurons controlling muscle activity of the vocal organ and others of which project to nuclei involved in respiratory control (Suthers and Margoliash 2002).

There is another connection between HVc and RA, a set of nuclei called the anterior forebrain pathway (AFP). The AFP does not participate in the production of song but plays a crucial role in learning and maintaining song (Brainard and Doupe 2002). The output of this pathway is from nucleus lMAN to RA. RA neurons receive inputs from both lMAN and HVc neurons, consistent with the picture that experience-related lMAN activity potentiates or depresses specific HVC $\rightarrow$ RA synapses, thus building the synaptic connectivity necessary to produce and maintain the adult song.

According to this picture, a sparse sequence of bursts generated in RA-projecting HVc neurons will evoke some activity in RA neurons, and signaling through the AFP will excite lMAN neurons. This lMAN signaling, however, requires a processing time through the AFP, which has been estimated at approximately 40–50 ms in adult male zebra finches (Troyer and Doupe 2000; Doupe 1997; Kimpo et al. 2003). Synaptic plasticity may depend on this time delay (Bi and Poo 2001; Malenka and Nicoll 1999), and that is what we explore here.

Correspondence to: H. D. I. Abarbanel
(e-mail: hdia@jacobi.ucsd.edu)

Many authors have suspected that alteration of synaptic strengths in RA is responsible for alteration of naive or learned song (Troyer and Doupe 2000; Stark and Perkel 1999; Mooney 1992). This suggestion is strengthened by the observation that signals from lMAN arrive at excitatory synapses on dendritic spines of RA neurons whose currents are mediated almost entirely by NMDA receptors (NMDARs), while signals from HVc arrive at excitatory synapses on dendritic spines of RA neurons whose currents are mediated by both NMDARs and AMPA receptors (AMPARs) (Stark and Perkel 1999). The idea that near coincidence of signals from these two pathways could lead to alterations in the strength of the AMPA conductance, and thus in the signaling through RA from HVc, is appealing (Mooney 1992).

The main role of the RA appears to be converting the sparse spatiotemporal patterns of HVc into the spatiotemporal patterns required for precise control of motor activity. We hypothesize in this paper that the plasticity in RA synaptic connections follows the same biophysical rules seen in mammalian preparations (Bi and Poo 2001; Malenka and Nicoll 1999), where timing-dependent learning rules are observed. RA projection neurons and interneurons receive inputs from both HVc and lMAN, so we must satisfy two conditions if this form of plasticity is to work: (1) the timing of the signals from HVc and from lMAN must lie within a relatively small window, or no synaptic strength change will occur; and (2) the events associated with signals from HVc and lMAN must be separated by a time of a syllable or more so that the signals with different instructions will not overlap. The former comes from our biophysical model, and the latter is achieved by sparseness of the HVc activity (Hahnloser et al. 2002) as both signals originate from HVc.

We have constructed a simple model of the biophysical induction (Abarbanel et al. 2003a) of synaptic plasticity, which describes quite well many observed LTP and LTD experiments on mammalian hippocampal and neocortical pyramidal neurons, where a mixture of NMDARs and AMPARs also plays a dynamical role. This model identifies the time course of elevated intracellular Ca^{2+} levels as responsible for the induction of synaptic plasticity. The change in plasticity is expressed in the model as an increase or decrease in conductance through AMPA channels on the postsynaptic neuron.

In this paper, we use this plasticity induction model to describe the changes in HVc $\rightarrow$ RA AMPA conductance as a function of the time delay ΔT between signals from HVc to RA and signals from lMAN to RA. In Fig. 1, we display a simplified version of the song system showing the HVc to RA part of the premotor pathway and the connections through the nuclei of the AFP. In Fig. 2, we show the timing structure of bursts from HVc and lMAN separated by ΔT. Because the signals from lMAN originate at HVc then traverse the AFP, $\Delta T > 0$. As a function of ΔT the change in HVc $\rightarrow$ RA AMPA connection strength (maximal conductance) Δg varies significantly in the region $\Delta T \approx 40$ ms, below which it is positive, leading to potentiation, and above which it is negative, leading to synaptic depression, or zero depending on the magnitude

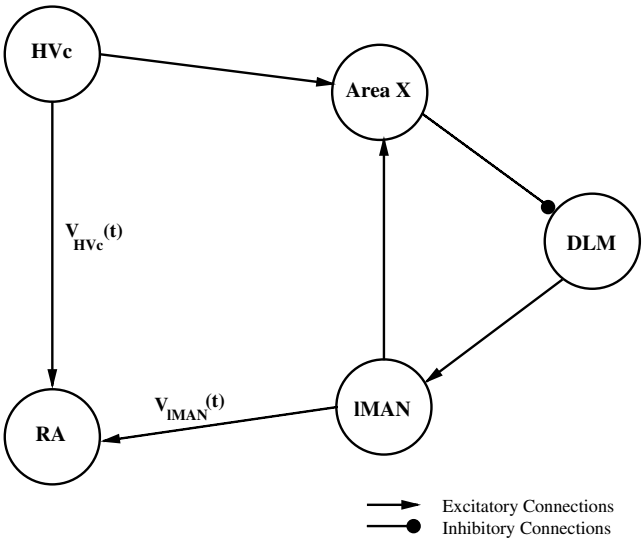

Fig. 1. A simplified representation of parts of the song system. In the premotor pathway we show the HVc and RA nuclei. In the anterior forebrain pathway (AFP) we show the Area X, DLM, and lMAN nuclei. Signals to RA come from HVc directly, and we show these as a voltage $V_{\mathrm{HVc}}(t)$ presynaptic to RA neurons, and they come through the AFP whose output is the lMAN nucleus. The signals that pass through the AFP are indicated by the voltage $V_{\mathrm{lMAN}}(t)$ presynaptic to RA neurons

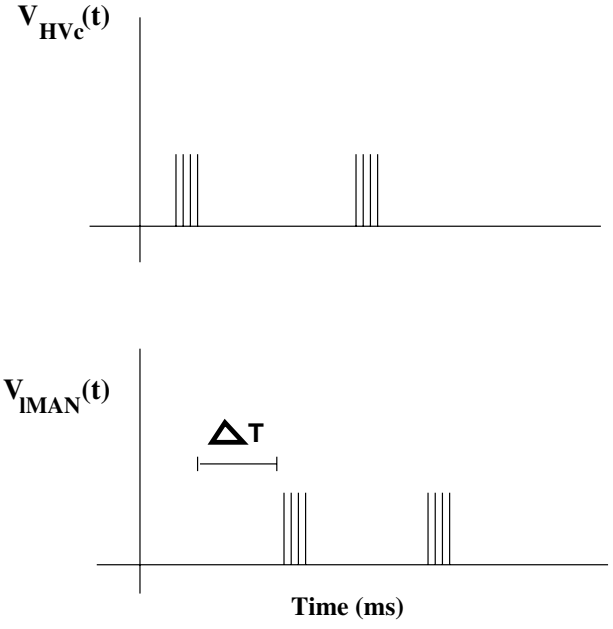

Fig. 2. A representation of the timing of HVc signals direct to RA and HVc signals that arrive at RA after passing through the AFP and exiting through lMAN

of ΔT. Building on the observations of Stark and Perkel (1999) we perform calculations of ΔT for combinations of NMDA and AMPA currents as seen in adult zebra finches and in juveniles.

We further examine the response of our biophysical model of plasticity as it is utilized in the setting just described. We present the RA nucleus with varying numbers of spikes from HVc and lMAN, first keeping the interspike

intervals (ISIs) fixed at 2 ms. Then we allow "noise" in the signaling by allowing the ISIs to vary uniformly around 2 ms with a 2-ms spread. This is consistent with the observations of (Hahnloser et al. 2002). In both of these cases, deterministic signaling and noisy signaling, a significant role is established for $\Delta T \approx 40$ ms. Finally, we explore the result of eliminating the influx of Ca^{2+} through the NMDARs receiving input from lMAN, and we show that this changes the picture substantially both with and without noisy ISIs.

2 The biophysical model

The mechanism of synaptic plasticity in our model is the change in intracellular Ca^{2+} concentration in an RA cell (Abarbanel et al. 2003a). This Ca^{2+} time course determines whether potentiation or depression is induced (Yang et al. 1999). We are interested here in the EPSPs created by the arrival of bursts of action potentials from HVc and lMAN, so we represent the RA neuron as a "passive" device operating near its resting potential of ≈ -70 mV. All changes in the RA membrane potential are induced by the arrival of action potentials from HVc and lMAN.

This model does not capture the dynamics of RA neurons in their "resting" state when no song is present. In that situation RA neurons projecting to either syrinx or respiratory control oscillate rather regularly at about 15–30 Hz while RA interneurons show small subthreshold variations (Yu and Margoliash 1996; Spiro et al. 1999; Leonardo 2002). When innervated by HVc signals, the RA projection neurons are broadly inhibited by these interneurons and show bursts of activity associated with the signals from HVc (and presumably through the AFP from lMAN). This means our calculations are focused on those epochs when the bird is singing, and we have implicitly presumed that this is when plasticity at the AMPA channels on the RA neurons is induced. When there is no song, we presume that signaling from lMAN is reduced or eliminated and autonomous activity in RA does not lead to substantial Δg.

To explore how the RA projection neurons dynamically end their tonic oscillations through global inhibition and experience plasticity driven by the Ca^{2+} dynamics discussed here, we would need a network model of the RA nucleus. We will present this in a future paper.

2.1 RA membrane voltage dynamics

We describe the passive RA neuron through its membrane potential $V_{\mathrm{RA}}(t)$ satisfying

$$C_{\mathrm{M}}\frac{\mathrm{d}V_{\mathrm{RA}}(t)}{\mathrm{d}t} = g_{\mathrm{L}}(V_{\mathrm{L}} - V_{\mathrm{RA}}(t)) + I_{\mathrm{HVc-NMDA}}(t) + I_{\mathrm{HVc-AMPA}}(t) + I_{\mathrm{lMAN-NMDA}}(t) + I_{\mathrm{lMAN-AMPA}}(t)\,, \quad (1)$$

where the "leak" current drives the neuron to $V_{\mathrm{RA}}(t) = V_{\mathrm{L}}$ in the absence of signaling from HVc or lMAN. C_{M} is the membrane capacitance per unit area.

The other synaptic currents are:

- The synaptic current through NMDARs into the RA cell in response to signals coming from HVc: $I_{\mathrm{HVc-NMDA}}(t) = g_{NH} S_{NH}(t|V_{\mathrm{HVc}}) B(V_{\mathrm{RA}}(t))(V_{\mathrm{NMDA-rev}} - V_{\mathrm{RA}}(t))$.
- The synaptic current through AMPARs into the RA cell in response to signals coming from HVc: $I_{\mathrm{HVc-AMPA}}(t) = g_{AH} S_A(t|V_{\mathrm{HVc}})(V_{\mathrm{AMPA-rev}} - V_{\mathrm{RA}}(t))$.
- The synaptic current through NMDARs into the RA cell in response to signals coming from lMAN: $I_{\mathrm{lMAN-NMDA}}(t) = g_{Nl} S_{Nl}(t|V_{\mathrm{lMAN}}) B(V_{\mathrm{RA}}(t))(V_{\mathrm{NMDA-rev}} - V_{\mathrm{RA}}(t))$.
- The synaptic current through AMPARs into the RA cell in response to signals coming from lMAN: $I_{\mathrm{lMAN-AMPA}}(t) = g_{Al} S_A(t|V_{\mathrm{lMAN}})(V_{\mathrm{AMPA-rev}} - V_{\mathrm{RA}}(t))$.

The maximal AMPA conductances g_{AH} and g_{Al} and the maximal NMDA conductances g_{NH} and g_{Nl} are constants. The variables $S_{NH}(t, V_{\mathrm{pre}}(t))$, $S_{Nl}(t, V_{\mathrm{pre}}(t))$, and $S_A(t, V_{\mathrm{pre}}(t))$ range between zero and unity and represent the fraction of NMDARs and AMPARs, respectively, that are open in response to the binding of glutamate. They are taken to satisfy

$$\frac{\mathrm{d}S_A(t|V_{\mathrm{pre}})}{\mathrm{d}t} = \frac{1}{\tau_A}\frac{S_0(V_{\mathrm{pre}}(t)) - S_A(t|V_{\mathrm{pre}})}{S_{1\mathrm{A}} - S_0(V_{\mathrm{pre}}(t))} \quad (2)$$

and

$$\frac{\mathrm{d}S_{Ni}(t|V_{\mathrm{pre}})}{\mathrm{d}t} = \frac{1}{\tau_{Ni}}\frac{S_0(V_{\mathrm{pre}}(t)) - S_{Ni}(t|V_{\mathrm{pre}})}{S_{1Ni} - S_0(V_{\mathrm{pre}}(t))} \quad i = 1, 2. \quad (3)$$

The two binding fractions for NMDARs allow us to reproduce the observed fast and slow decay times of NMDA currents (Stark and Perkel 1999). We write

$$S_{NH}(t|V_{\mathrm{HVc}}) = w_{\mathrm{H}} S_{N1}(t|V_{\mathrm{HVc}}) + (1 - w_H) S_{N2}(t|V_{\mathrm{HVc}}) \quad (4)$$

and

$$S_{Nl}(t|V_{\mathrm{lMAN}}) = w_l S_{N1}(t|V_{\mathrm{lMAN}}) + (1 - w_l) S_{N2}(t|V_{\mathrm{lMAN}}). \quad (5)$$

In these expressions, $S_0(V_{\mathrm{pre}})$ rises rapidly from zero as a presynaptic action potential from HVc or lMAN arrives then falls again to zero after the passage of presynaptic activity. For $S_0(V)$ we use the "step function"

$$S_0(V) = \frac{1}{2}(1 + \tanh(120(V - 0.1)))\,. \quad (6)$$

The constants τ_A and S_{1A} are chosen so that AMPA currents rise in approximately 0.1 ms and decay in 1.4 ms. For the NMDA currents from lMAN we choose $\tau_{N1} = 29$ ms, $S_{1N1} = 30/29$, $\tau_{N2} = 139$ ms, and $S_{1N2} = 140/139$. For the NMDA currents from HVc we choose $\tau_{N1} = 19$ ms, $S_{1N1} = 20/19$, $\tau_{N2} = 99$ ms, and $S_{1N2} = 100/99$. For lMAN NMDA currents the weight is $w_l = 0.41$, while for HVc NMDA currents we choose $w_H = 0.32$. This leads to NMDA channel time courses consistent with the observations of Stark and Perkel (1999).

It has long been known that NMDA channels are blocked in a voltage-dependent manner by magnesium ions (Hille 2001; Nowak et al. 1984; Mayer et al. 1984). The factor $B(V)$ in the NMDA currents expresses this feature of the dynamics. Its form is

$$B(V) = \frac{1}{1 + 0.288[\mathrm{Mg}^{2+}]\mathrm{e}^{-0.062V}}, \tag{7}$$

where the concentration of extracellular magnesium $[\mathrm{Mg}^{2+}]$ is in units of mM and the voltage is in units of mV. We routinely use $[\mathrm{Mg}^{2+}] = 1$. In the paper of Zhang et al. (1997) it is noted that a "normal" extracellular Mg^{2+} concentration is 1.2 mM, and numbers in the range of 0.5–1.5 mM are standard. In Abarbanel et al. (2003a) we explored the effect of changing this quantity on the synaptic plasticity results. For variations in the range of $\approx 20\%$ around 1.0 mM, little changed. As this concentration becomes very small, of course, the block of NMDARs is removed and LTD is no longer seen.

2.2 Intracellular Ca^{2+} in RA neurons

These AMPA and NMDA currents lead to changes in the intracellular concentration of Ca^{2+}, which we denote by $Ca(t)$. The Ca^{2+} dynamics are taken to be

$$\frac{\mathrm{d}Ca(t)}{\mathrm{d}t} = \frac{C_0 - Ca(t)}{\tau_C} + C_{\mathrm{HVc-NMDA}}(t) + C_{\mathrm{HVc-AMPA}}(t) + C_{\mathrm{lMAN-NMDA}}(t) + C_{\mathrm{lMAN-AMPA}}(t), \tag{8}$$

where the first term represents an intracellular relaxation process for Ca^{2+} with a time constant $\tau_C \approx 25$ ms (Sabatini et al. 2001, 2002). The other Ca^{2+} currents are:

- The Ca^{2+} current through NMDARs into the RA cell in response to signals coming from HVc: $C_{\mathrm{HVc-NMDA}}(t) = g_{NC} S_{NH}(t|V_{\mathrm{HVc}}) B(V_{\mathrm{RA}}(t))(V_{\mathrm{NMDA-rev}} - V_{\mathrm{RA}}(t))$.
- The Ca^{2+} current through AMPARs into the RA cell in response to signals coming from HVc: $C_{\mathrm{HVc-AMPA}}(t) = g_{AC} S_A(t|V_{\mathrm{HVc}})(V_{\mathrm{AMPA-rev}} - V_{\mathrm{RA}}(t))$.
- The Ca^{2+} current through NMDARs into the RA cell in response to signals coming from lMAN: $C_{\mathrm{lMAN-NMDA}}(t) = g_{NC} S_{Nl}(t|V_{\mathrm{lMAN}}) B(V_{\mathrm{RA}}(t))(V_{\mathrm{NMDA-rev}} - V_{\mathrm{RA}}(t))$.
- The Ca^{2+} current through AMPARs into the RA cell in response to signals coming from lMAN: $C_{\mathrm{lMAN-AMPA}}(t) = g_{AC} S_A(t|V_{\mathrm{lMAN}})(V_{\mathrm{AMPA-rev}} - V_{\mathrm{RA}}(t))$.

We prescribe patterns of HVc bursts of spikes → RA in the voltage $V_{\mathrm{HVc}}(t)$ presynaptic to RA and patterns of lMAN bursts of spikes → RA in the voltage $V_{\mathrm{lMAN}}(t)$ presynaptic to RA. This allows us to determine $V_{\mathrm{RA}}(t)$ by (1), and from that we evaluate $Ca(t)$ in the postsynaptic RA cell from the dynamics of (8). In this paper, we do not make a model of either AFP or HVc dynamics.

2.3 Changes in g_A at HVC → RA connections

The role of Ca^{2+} in synaptic plasticity has led to the identification of various metabolic pathways involving kinases that phosphorylate and phosphatases that dephosphorylate distinct sites on the AMPAR (Lee et al. 2000) and perhaps lead to the recruitment of previously "silent" AMPARs that are delivered to the postsynaptic density (Malenka and Nicoll 1999; Malinow and Malenka 2002). We have simplified the kinetics of these processes, part of which are discussed in more detail in Castellani et al. (2001), to a coupled set of first-order kinetic equations for activity $D(t)$, which leads to the phosphorylation or addition of AMPARs, and activity $P(t)$, which leads to the dephosphorylation or removal of AMPARs. These satisfy

$$\begin{aligned} \frac{\mathrm{d}P(t)}{\mathrm{d}t} &= f_P(Ca(t) - C_0)(1 - P(t)) - \frac{P(t)}{\tau_P}, \\ \frac{\mathrm{d}D(t)}{\mathrm{d}t} &= f_D(Ca(t) - C_0)(1 - D(t)) - \frac{D(t)}{\tau_D}, \end{aligned} \tag{9}$$

where $f_P(x)$ and $f_D(x)$ are driving functions for the dynamics dependent on the perturbation of Ca^{2+} from its equilibrium value C_0. We take these functions to have Hill forms

$$\begin{aligned} f_P(x) &= \frac{x^L}{\Gamma_{\mathrm{P}} + x^L}, \\ f_D(x) &= \frac{x^M}{\Gamma_{\mathrm{D}} + x^M}, \end{aligned} \tag{10}$$

where L and M are integers ranging between 2 and 8 in our simulations. The same form of driving function has been used by Zhabotinsky (2000) and is a familiar saturating form of forcing with a saturation threshold determined by the dissociation constants Γ_D or Γ_P.

When $Ca(t) - C_0$ deviates from zero, these kinetic equations drive $P(t)$ and $D(t)$ from their rest state of zero. This "rest" state is the normal equilibrium of the cell where the competition among such processes has resulted in an AMPA conductance g_A. The time constants associated with these processes are taken to be those seen in the spike-timing plasticity experiments and are nominally $\tau_P \approx 10$ ms and $\tau_D \approx 30$ ms.

Our critical assumption is based on our phenomenological description of spike-timing plasticity (Abarbanel et al. 2002). It relates the change in AMPA conductance, Δg, to a specific form of nonlinear competition between these two processes:

$$\frac{\mathrm{d}\Delta g(t)}{\mathrm{d}t} = g_A \gamma \{P(t)D(t)^\eta - D(t)P(t)^\eta\}. \tag{11}$$

The parameters we used in our modeling were $C_M = 1\mu\mathrm{F/cm}^2$, $g_L = 0.08\,\mathrm{mS/cm}^2$, and $g_{AC} = 1.5 \times 10^{-4}\,\mathrm{mS/cm}^2$. The reversal potentials for the excitatory NMDA and AMPA channels are $0\,\mathrm{mV/cm}^2$. $V_L = -70.4$ mV. In the phenomenological model we take $L = 4$ and $M = 8$, and $\Gamma_P = \xi^L$ and $\Gamma_D = \xi^M$. We choose $\xi = 6.5$, $\tau_P = 12$ ms, and $\tau_D = 30$ ms. Our mechanism only describes the *induction* of plasticity. The actual changes in synaptic strength may occur over times much longer than the tens of milliseconds required for induction.

For both adult and juvenile birds, we selected $g_{NH} = g_N/2$, $g_{AH} = g_A$, $g_{Nl} = g_N$, and $g_{Al} = g_A/10$. For adult

birds, we chose $g_N = g_A = 0.05\,\mathrm{mS/cm^2}$, while for juveniles, we selected $g_N = 0.1\,\mathrm{mS/cm^2}$ and $g_A = 0.05\,\mathrm{mS/cm^2}$. The values of g_{NC} were varied in each case over a small range to assure that when the HVc bursts and lMAN bursts were separated in time by much more than 150 ms, the change in synaptic strength was zero. The particular values used are given in the captions to the figures in the next section.

3 Results

Our calculations consist of presenting the RA neuron, described by its membrane voltage $V_{\mathrm{RA}}(t)$ and its intracellular Ca^{2+} concentration $Ca(t)$, with two bursts of presynaptic spikes. One burst comes from HVc and influences the RA neuron via AMPARs [$I_{\mathrm{HVc-AMPA}}(t)$] and NMDARs [$I_{\mathrm{HVc-NMDA}}(t)$]. The other set, delayed by a time interval ΔT (Fig. 2), comes from lMAN and influences the RA neuron via NMDARs [$I_{\mathrm{lMAN-NMDA}}(t)$] and AMPARs as well [$I_{\mathrm{lMAN-AMPA}}(t)$]. The presynaptic spike bursts from HVc and lMAN influence RA through $S_{NH}(t|V_{\mathrm{HVc}})$, $S_{Nl}(t|V_{\mathrm{lMAN}})$, and $S_A(t|V_{\mathrm{pre}})$ only.

The first calculations we performed were deterministic, with fixed interspike intervals (ISIs) in each burst of spikes. We presented the RA neuron with a burst of N_{HVc} spikes from HVc with ISIs of 2 ms. At ΔT after the HVc burst ended, we presented the RA neuron with a burst of N_{lMAN} spikes from lMAN, and also with ISI = 2 ms. In Fig. 3, we show the result for $\Delta g/g_A$ as a function of ΔT when $N_{\mathrm{HVc}} = N_{\mathrm{lMAN}} = 3$. To determine $\Delta g/g_A$ we first evaluated $V_{\mathrm{RA}}(t)$ due to these presynaptic actions. From $V_{\mathrm{RA}}(t)$ we evaluated the intracellular Ca^{2+} concentration time course $Ca(t)$. Using $Ca(t)$ we determined $\Delta g/g_A$. In the phenomenological equation for $\Delta g/g_A$ we used $\eta = 4$ and $\gamma = 15$ (Abarbanel et al. 2003a). For ΔT much greater than 120 ms, $\Delta g/g_A$ is essentially zero.

This suggests the possibility that there is a temporal window near $\Delta T \approx 40$ ms in the plasticity of HVc → RA connections where the sign of synaptic strength change is sensitive to the time difference between HVc spiking and lMAN spiking. When ΔT is too large, no further change occurs.

In Fig. 4, we present the same calculation with $N_{\mathrm{HVc}} = N_{\mathrm{lMAN}} = 5$. Again we see the important role of values of ΔT near 40 ms.

The observations of Hahnloser et al. (2002) show that the RA-projecting HVc neurons produce bursts of 4.5 ± 2 spikes lasting 6.1 ± 2 ms, and we have chosen our ISI values in accordance with these measurements. There are no data to tell us what the lMAN → RA signals should be, but we assumed that they resemble the HVc → RA bursts. In each of the cases with $N_{\mathrm{HVc}} = N_{\mathrm{lMAN}}$ we see potentiation for $\Delta T \approx 40$ ms or less, then a region of depression until $\Delta T \approx 100$ ms, and finally no change in g_A for larger values of ΔT. The precise values of ΔT where one sees potentiation end, depression begin, and then $\Delta g/g_A = 0$ take over differ in detail from case to case, but the overall pattern is the same. The role of $\Delta T \approx 40$ ms is clear in each instance.

Quite similar behavior for $\Delta g/g_A$ is seen when we select $N_{\mathrm{HVc}} = 5$ and $N_{\mathrm{lMAN}} = 3$, as shown in Fig. 5, and for $N_{\mathrm{HVc}} = 3$ and $N_{\mathrm{lMAN}} = 5$ in Fig. 6. The important role of time delays in the neighborhood of ΔT near 40 ms remains clear.

We inquired into the robustness of this result when there is noise or natural variation in the ISIs of the presynaptic spiking. Noise in each burst of spikes was represented by choosing the ISIs from a uniform distribution of ISIs with mean 2 ms and RMS variation 1 ms, so ISIs between 1 and

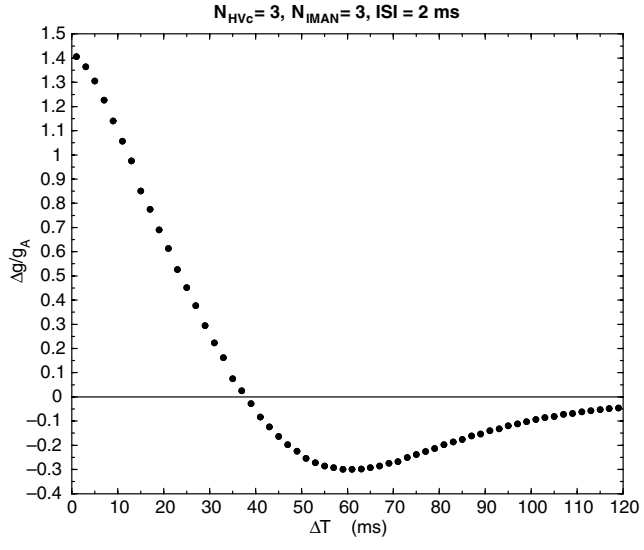

Fig. 3. $\Delta g/g_A$, the fractional change in HVc → RA AMPA conductance, for $N_{\mathrm{HVc}} = N_{\mathrm{lMAN}} = 3$ as a function of ΔT, the time delay between the arrival of the HVc burst and the lMAN burst. Near $\Delta T \approx 40$ ms the sign of Δg changes from positive (potentiation) to negative (depression). For $\Delta T \leq 35$ ms, only potentiation appears. $g_{NC} = 0.061\,\mathrm{mS/cm^2}$

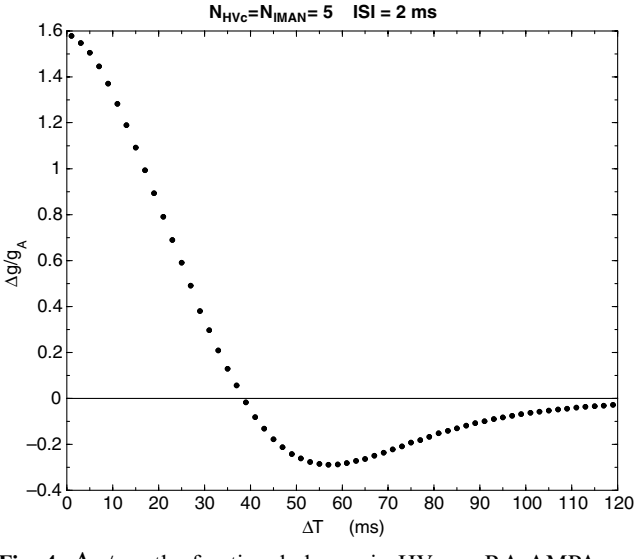

Fig. 4. $\Delta g/g_A$, the fractional change in HVc → RA AMPA conductance, for $N_{\mathrm{HVc}} = N_{\mathrm{lMAN}} = 5$ as a function of ΔT, the time delay between the arrival of the HVc burst and the lMAN burst. The ISIs in the bursts of spikes are all 2 ms. Near $\Delta T \approx 40$ ms the sign of Δg changes from positive (potentiation) to negative (depression). $g_{NC} = 0.051\,\mathrm{mS/cm^2}$

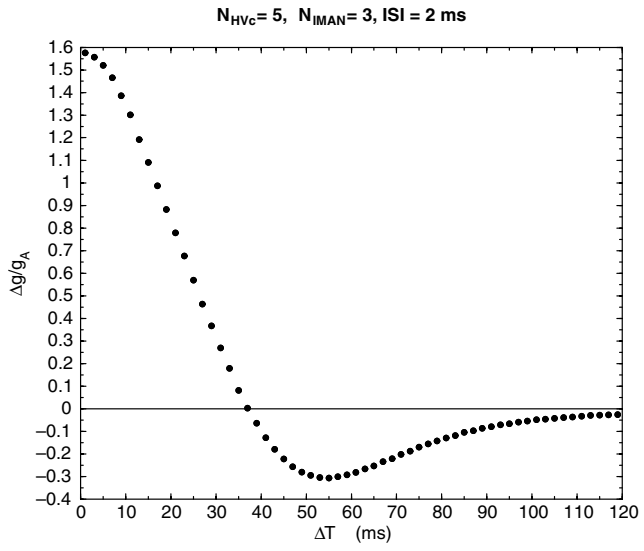

Fig. 5. $\Delta g/g_A$, the fractional change in HVc → RA AMPA conductance for $N_{\mathrm{HVc}} = 5$ and $N_{\mathrm{lMAN}} = 3$ as a function of ΔT, the time delay between the arrival of the HVc spike and the lMAN spike. The ISIs in the bursts of spikes are each 2 ms. Near $\Delta T \approx 40$ ms the sign of Δg changes from positive (potentiation) to negative (depression). $g_{NC} = 0.055$ mS/cm^2

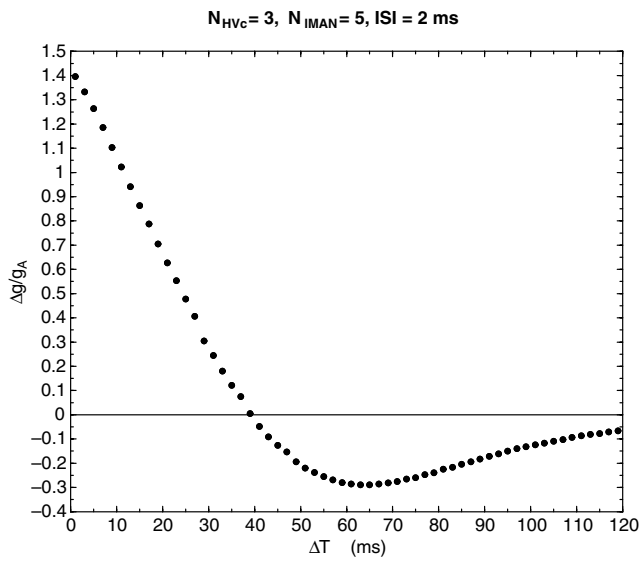

Fig. 6. $\Delta g/g_A$, the fractional change in HVc → RA AMPA conductance, for $N_{\mathrm{HVc}} = 3$ and $N_{\mathrm{lMAN}} = 5$ as a function of ΔT, the time delay between the arrival of the HVc burst and the lMAN burst. The ISIs in the bursts of spikes are all 2 ms. Near $\Delta T \approx 40$ ms the sign of Δg changes from positive (potentiation) to negative (depression). $g_{NC} = 0.056$ mS/cm^2

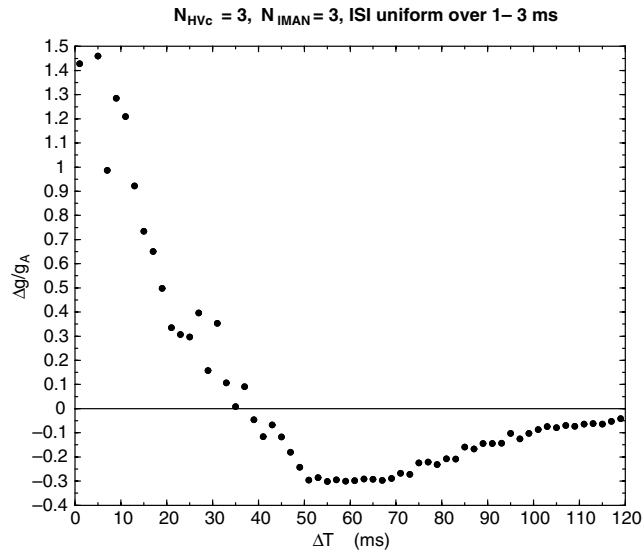

Fig. 7. $\Delta g/g_A$, the fractional change in HVc → RA AMPA conductance, for $N_{\mathrm{HVc}} = N_{\mathrm{lMAN}} = 3$ as a function of ΔT, the time delay between the arrival of the HVc burst and the lMAN burst. The ISIs in the bursts of spikes are selected from a uniform distribution with mean 2 ms and RMS variation 1 ms. The main features of the noise-free case remain unchanged. $g_{NC} = 0.061$ mS/cm^2

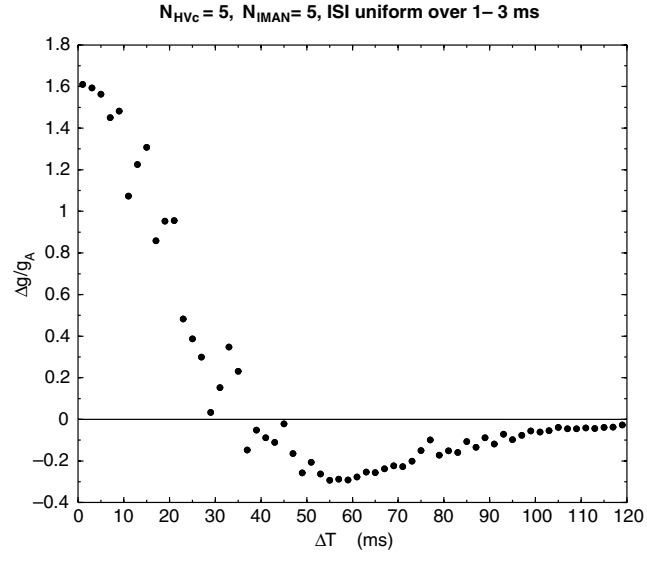

Fig. 8. $\Delta g/g_A$, the fractional change in HVc → RA AMPA conductance, for $N_{\mathrm{HVc}} = N_{\mathrm{lMAN}} = 5$ as a function of ΔT, the time delay between the arrival of the HVc burst and the lMAN burst. The ISIs in the bursts of spikes are selected from a uniform distribution with mean 2 ms and RMS variation 1 ms. The main features of the noise-free case remain unchanged. $g_{NC} = 0.051$ mS/cm^2

3 ms appear with uniform probability. Again, this range of ISIs is in accordance with the observations (Hahnloser et al. 2002).

In Fig. 7, we show the result of this addition of noise for the case when $N_{\mathrm{HVc}} = N_{\mathrm{lMAN}} = 3$. It is clear that the importance of the region near $\Delta T \approx 40$ ms remains. Choosing $N_{\mathrm{HVc}} = N_{\mathrm{lMAN}} = 5$ and adding the same noise produces the result shown in Fig. 8, again indicating the robustness of our observation to variations in the ISIs of the spikes in the presynaptic bursts presented to RA neurons.

The results presented thus far assume that the Ca^{2+} entering at both HVc → RA and lMAN → RA spines contributes to plasticity. Next we asked what would happen if we removed the contribution of the Ca^{2+} that enters through lMAN → RA NMDARs.

In Fig. 9, we show the outcome of our model for $\Delta g/g_A$ when $N_{\mathrm{HVc}} = N_{\mathrm{lMAN}} = 3$ and the Ca^{2+} contribution

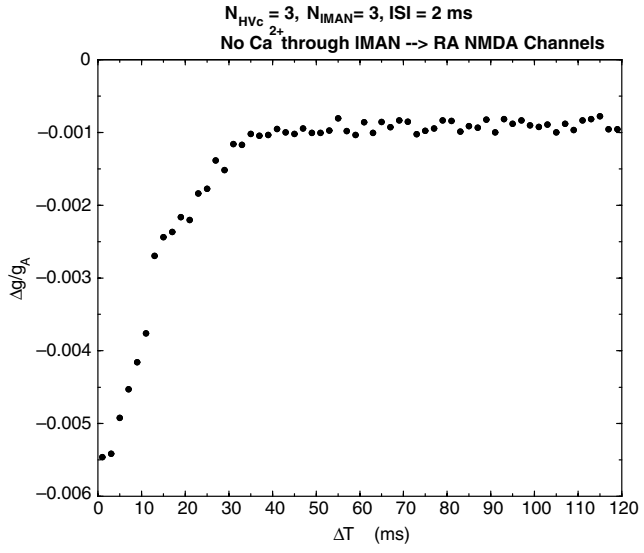

Fig. 9. $\Delta g/g_A$, the fractional change in HVc → RA AMPA conductance, for $N_{\mathrm{HVc}} = N_{\mathrm{lMAN}} = 3$ as a function of ΔT, the time delay between the arrival of the HVc burst and the lMAN burst. In this result we blocked the Ca^{2+} influx through the NMDARs responsive to lMAN spikes. As one can see, this blocking of Ca^{2+} influx removes LTP altogether and reduces the overall effect on synaptic plasticity significantly. The ISIs are fixed at 2 ms

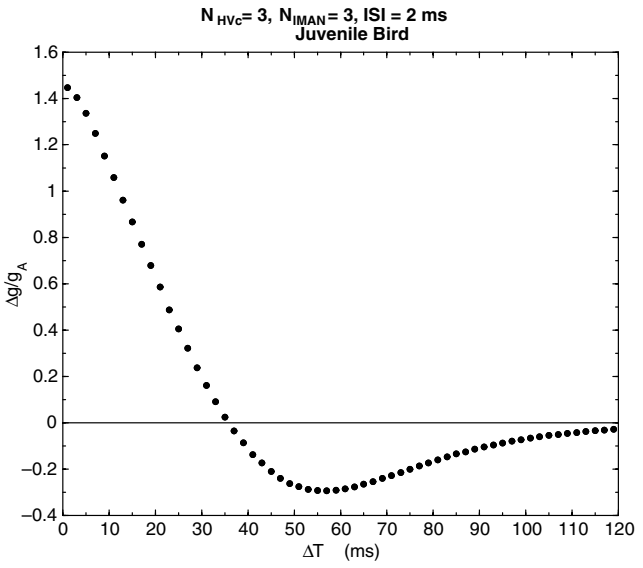

Fig. 10. The fractional change in AMPA conductance at the HVc → RA junction when $N_{\mathrm{HVc}} = N_{\mathrm{lMAN}} = 3$. The NMDA to AMPA ratio at this junction is set to 2.0, as suggested by the observations of Stark and Perkel (1999) for juvenile and fledgling birds. The ISIs are fixed at 2 ms. $g_{NC} = 0.056\,\mathrm{mS/cm^2}$

of lMAN → RA NMDARs is removed. Removing this source of Ca^{2+} eliminates LTP altogether and gives only a shallow LTD for all ΔT. With other choices of N_{HVc} and N_{lMAN} the result is quite similar, and adding noise to the ISIs does not change the outcome.

Stark and Perkel (1999) demonstrate that the NMDA to AMPA ratio in the HVc → RA connections differs in the adult, juvenile, and fledgling birds. In the latter the ratio is near 2, while in the adult bird it is nearer to unity. In the calculations presented above, we have used 1.0 for this ratio. We have also done the calculations of $\Delta g/g_A$ as a function of ΔT for this ratio set to 2.0, as in the juvenile and fledgling birds. In Fig. 10 we show the result of this calculation when we have $N_{\mathrm{HVc}} = N_{\mathrm{lMAN}} = 3$, and in Fig. 11 $N_{\mathrm{HVc}} = N_{\mathrm{lMAN}} = 5$. There is no substantial difference in the behavior of $\Delta g/g_A$ for this ratio of NMDA to AMPA conductances in either case. Similarly, when we add noise to the ISIs, as above, the variations about the deterministic curves presented are small.

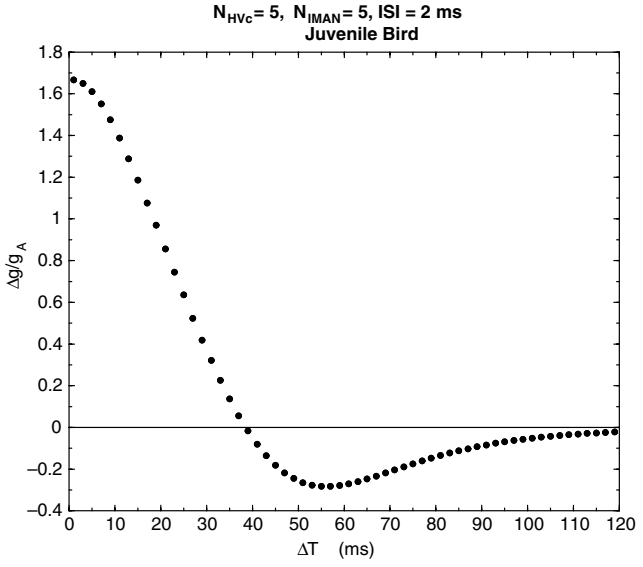

Fig. 11. $\Delta g/g_A$, the fractional change in HVc → RA AMPA conductance, for $N_{\mathrm{HVc}} = N_{\mathrm{lMAN}} = 5$ as a function of ΔT, the time delay between the arrival of the HVc burst and the lMAN burst. In this calculation the NMDA to AMPA strength ratio of 2.0 appropriate to juvenile and fledgling birds (Stark and Perkel 1999) was used. The ISIs are fixed at 2 ms. $g_{NC} = 0.047\,\mathrm{mS/cm^2}$

4 Discussion

Guided by experimental observations about the synaptic connections in RA from HVc and from the AFP through lMAN (Mooney 1992; Stark and Perkel 1999), we have built a model of synaptic plasticity for HVc → RA synaptic connections through ligand-gated AMPA receptors. It is observed (Yu and Margoliash 1996; Spiro et al. 1999; Leonardo 2002) that when there is no production of song, i.e., the signaling from HVc directly to RA and indirectly through the AFP to RA is absent, the RA projection neurons oscillate regularly at 15–30 Hz. The RA interneurons are nearly silent with some small subthreshold activity during this period. When the bird produces song, the RA projection neurons exit from the tonic oscillations and produce sparse bursts of spikes associated with HVc activity. One may presume they are globally inhibited by the inhibition from the interneurons that are also innervated by HVc activity. Our model focuses on this song production period where we have assumed that HVc direct innervation of RA neurons coordinated with indirect innervation through the AFP and lMAN, as the AFP's output nucleus, leads to synaptic plasticity in RA.

The model describes RA membrane voltage activity near the resting potential and ascribes changes in AMPA strength to the time course of intracellular Ca^{2+} concentration induced by signals received by RA from HVc and lMAN, through AMPARs and NMDARs. The model was constructed using as its critical ingredient the description we have explored (Abarbanel et al. 2003a) of plasticity at mammalian hippocampal and neocortical synapses.

Let us say a word about the critical parameters in our model. The synaptic plasticity model has been explored in (Abarbanel et al. 2003a), where the constants entering the phenomenological connection between elevation of intracellular Ca^{2+} and increase in AMPA conductance were set to be consistent with observations. The only changes here from the model explored there is the elimination of degrees of freedom in the RA cell that might lead to spiking, namely, Na, K, and leak dynamics typical of HH models, changes in the distribution of NMDA and AMPA receptors to reflect the observations of Stark and Perkel (1999), and, finally, small adjustments in the Ca^{2+} conductivity of NMDARs to assure that when ΔT is large, Δg_A goes to zero. One could make major changes in the RA cellular properties, including allowing it to spike (unpublished calculations by the authors), but the EPSPs near rest are the critical determinants of the elevation of intracellular Ca^{2+} that leads to synaptic changes. Indeed, as long as one respects the time course of Ca^{2+} elevation due to spikes received from lMAN and HVc, the synaptic plasticity rule from Abarbanel et al. (2003a) appears to yield a region of $\Delta g_A \approx 0$ near $\Delta T \approx 40$ ms regardless of the details of how that Ca^{2+} elevation is induced. Most of the biophysical parameters used here are set by observations: the time constants for NMDARs and AMPARs, the ratio of AMPARs and NMDARs at the HVc to RA and lMAN to RA junctions, the form of the Mg^{2+} voltage block of NMDARs, etc. The critical freedom is in the Ca^{2+} flux equation, (8), where we have two permeabilities g_{NC} and g_{AC} to set. The latter is small and could be eliminated; the former is essential.

We can make contact with the observations of Leonardo and Konishi (1999) and Leonardo (2002), in which the auditory feedback from vocalization in adult male zebra finches was perturbed by additional acoustic signals. In our model, such perturbations would be represented as changes in the delay, ΔT. This would lead to changes in the premotor HVc $\rightarrow$ RA synaptic strengths and reversible changes in the song. Similarly, the ideas explored here are consistent with the observations of Brainard and Doupe (2000) and Williams and Mehta (1999) that lesioning AFP nuclei and deafening the bird prevent the song disruption associated with deafening alone. In this case, the time ΔT would be effectively infinite, and thus $\Delta g = 0$.

It is necessary to test these statements with a model of the AFP, and we have been developing such a model based on electrophysiological observations about the various nuclei (Area X, DLM, and lMAN) in that pathway (Abarbanel et al. 2003b; Luo and Perkel 2002; Perkel et al. 2002; Brainard and Doupe 2002). This model exhibits a delay of HVc $\rightarrow$ Area X $\rightarrow$ DLM $\rightarrow$ LMAN $\rightarrow$ RA signals relative to HVc $\rightarrow$ RA signals. The inhibitory connections between Area X and DLM play an important role in the AFP dynamics described by the model (Abarbanel et al. 2003b).

Our results suggest a quantitative interpretation of the way in which signals from the AFP are used in learning birdsong. If learning involves changes in synaptic strength in the premotor HVc $\rightarrow$ RA pathway, then it depends on the magnitude of ΔT, the delay between HVc and lMAN signaling to RA. A picture of crystallization of song also emerges. This focuses on ΔT as the critical parameter that must be adjusted by the operation of the AFP nuclei. The adjustment of the ΔT's associated with the many connections from lMAN to RA would be seen as the actual task in learning song in the sensorimotor phase and in maintaining it as an adult. Mechanisms for learning from a tutor in the sensory phase are not informed by the model we have at present. How ΔT may be modulated within the AFP is a matter for further investigation, though the sensitivity to the inhibitory input from Area X to DLM (Luo and Perkel 2002) and the possibility of modulation of Area X and lMAN neurons by dopamine (Ding and Perkel 2002; Ding et al. 2003) are attractive candidates for this role (Abarbanel et al. 2003b).

Acknowledgements. This work was partially funded by UBA, Fundacion Antorchas supporting GBM; by the US Department of Energy, Office of Basic Energy Sciences, Division of Engineering and Geosciences, under Grant Nos. DE-FG03-90ER14138 and DE-FG03-96ER14592 supporting HDIA and MIR; by a grant from the National Science Foundation, NSF PHY0097134 supporting LG; and by a grant from the National Institutes of Health, NIH R01 NS40110-01A2 supporting ST and HDIA.

References

Abarbanel HDI, Huerta R, Rabinovich MI (2002) Dynamical model of long-term synaptic plasticity. Proc Natl Acad Sci USA 99:10132–10137

Abarbanel HDI, Gibb L, Huerta R, Rabinovich MI (2003a) Biophysical model of synaptic plasticity dynamics. Biol Cybern 89:214–226

Abarbanel HDI, Gibb L, Mindlin GB, Rabinovich MI, Talathi S (2003b) Dynamics of the anterior forebrain pathway in birdsong control and learning. (accepted), Phys. Rev. E (in press)

Bi GQ, Poo MM (2001) Synaptic modification by correlated activity: Hebb's postulate revisited. Annu Rev Neurosci 24:139–166

Brainard MS, Doupe AJ (2000) Interruption of a basal ganglia-forebrain circuit prevents plasticity of learned vocalizations. Nature 404:762–766

Brainard MS, Doupe AJ (2002) What songbirds teach us about learning. Nature 417:351–358

Brenowitz EA, Margoliash D, Nordeen KW (1997) An introduction to birdsong and the avian song system. J Neurobiol 33:495–500

Castellani GC, Quinlan EM, Cooper LN, Shouval HZ (2001) A biophysical model of bidirectional synaptic plasticity: dependence on AMPA and NMDA receptors. Proc Natl Acad Sci USA 98:12772–12777

Ding L, Perkel DJ (2002) Dopamine modulates excitability of spiny neurons in the avian basal ganglia. J Neurosci 22:5210–5218

Ding L, Perkel DJ, Farries MA (2003) Presynaptic depression of glutamatergic synaptic transmission by D1-like dopamine receptor activation in the avian basal ganglia. J Neurosci 23:6086–6095

Doupe AJ (1997) Song- and order-selective neurons in the songbird anterior forebrain and their emergence during vocal development. J Neurosci 17:1147–1167

Hahnloser RH, Kozhevnikov AA, Fee MS (2002) An ultra-sparse code underlies the generation of neural sequences in a songbird. Nature 419:65–70

Hille B (2001) Ion Channels of excitable membranes, 3rd edn. Sinauer Associates, Sunderland, MA

Kimpo RR, Theunissen FE, Doupe AJ (2003) Propagation of correlated activity through multiple stages of a neural circuit. J Neurosci 23:5750–5761

Konishi M (1965) The role of auditory feedback in the control of vocalization in the white-crowned sparrow. Z Tierpsychol 22:770–783

Konishi M (1985) Birdsong: from behavior to neuron. Annu Rev Neurosci 8:125–170

Lee HK, Barbarosie M, Kameyama MK, Bear MF, Huganir RL (2000) Regulation of distinct AMPA receptor phosphorylation sites during bidirectional synaptic plasticity. Nature 405: 955–959

Leonardo A (2002) Neural dynamics underlying complex behavior in a songbird. PhD Dissertation, California Institute of Technology, Pasadena, CA

Leonardo A, Konishi M (1999) Decrystallization of adult birdsong by perturbation of auditory feedback. Nature 399:199–207

Luo M, Perkel DJ (2002) Intrinsic and synaptic properties of neurons in an avian thalamic nucleus during song learning. J Neurophysiol 88:1903–1914

Malenka RC, Nicoll RA (1999) Long-term potentiation—a decade of progress? Science 285:1870–1874

Malinow R, Malenka RC (2002) AMPA receptor trafficking and synaptic plasticity. Annu Rev Neurosci 25:103–126

Mayer ML, Westbrook GL, Guthrie PB (1984) Voltage-dependent block by Mg^{2+} of NMDA responses in spinal cord neurones. Nature 309:261–263

Mooney R (1992) Synaptic basis for developmental plasticity in a birdsong nucleus. J Neurosci 12:2464–2477

Nottebohm F (2002) Birdsong's clockwork. Nat Neurosci 5: 925–926

Nowak L, Bregestovski P, Ascher P, Hebet A, Prochiantz A (1984) Magnesium gates glutamate-activated channels in mouse central neurones. Nature 307:462–465

Perkel DJ, Farries MA, Luo M, Ding L (2002) Electrophysiological analysis of a songbird basal ganglia circuit essential for vocal plasticity. Brain Res Bull 57:529–532

Sabatini BL, Maravall M, Svoboda K (2001) Ca^{2+} signaling in dendritic spines. Curr Opin Neurobiol 11:349–356

Sabatini BL, Oertner TG, Svoboda K (2002) The life cycle of Ca^{2+} ions in dendritic spines. Neuron 33:439–452

Spiro JE, Dalva MB, Mooney RJ (1999) Long-range inhibition within the zebra finch song nucleus RA can coordinate the firing of multiple projection neurons. J Neurophysiol 81:3007–3020

Stark LL, Perkel DJ (1999) Two-stage, input-specific synaptic maturation in a nucleus essential for vocal production in the zebra finch. J Neurosci 19:9107–9116

Suthers RA, Margoliash D (2002) Motor control of birdsong. Curr Opin Neurobiol 12:684–690

Troyer TW, Doupe AJ (2000) An associational model of birdsong sensorimotor learning: I. Efference copy and the learning of song syllables. J Neurophysiol 84:1204–1223

Williams H, Mehta N (1999) Changes in adult zebra finch song require a forebrain nucleus that is not necessary for song production. J Neurobiol 39:14–28

Yang S-N, Tang Y-G, Zucker RS (1999) Selective induction of LTP and LTD by postsynaptic $[Ca^{2+}]$ elevation. J Neurophysiol 81:781–787

Yu AC, Margoliash D (1996) Temporal hierarchical control of singing in birds. Science 273:1871–1875

Zhabotinsky AM (2000) Bistability in the Ca^{2+}/calmodulin-dependent protein kinase-phosphatase system. Biophys J 79: 2211–2221

Zhang A, Altura BT, Altura BM (1997) Elevation of extracellular magnesium rapidly raises intracellular free Mg^{2+} in human aortic endothelial cells: is extracellular Mg^{2+} a regulatory cation? Front Biosci 2:13–17